FIZIKA 9 (1977) Supplement 4, 513–558
(Proceedings of the Int. Symp. on Nuclear Collisions and
Their Microscopic Description, Bled, September 1977)

Relaxation Phenomena in Deeply Inelastic Heavy Ion Collisions[+)]

Georg Wolschin

Institut für theoretische Physik der Universität and
Max-Planck-Institut für Kernphysik, Heidelberg

Mass transfer, energy and angular momentum dissipation in deeply inelastic collisions between heavy nuclei are investigated in a transport theoretical approach. The Fokker-Planck equation as an approximation of the master equation for the internal degrees of freedom is discussed in detail, together with a microscopic model for the calculation of drift and diffusion coefficients. Analytic expressions for these transport coefficients are derived. Combining the theoretical results with the mean interaction times obtained in an analysis of experimental data, we calculate element distributions as well as mean value and variance of the dissipated angular momentum. Good agreement with recent experimental element distributions and γ-ray multiplicity data is obtained.

+) Work supported by the "Gesellschaft für Schwerionenforschung", Darmstadt, and the "Bundesministerium für Forschung und Technologie", Bonn.

1. Introduction

Deeply inelastic collisions between heavy nuclei offer a unique possiblity to study relaxation processes in a small quantum system. Although the identity of projectile and target is essentially preserved in these reactions, a large amount of mass can be transferred, the relative kinetic energy is dissipated and relative angular momentum is transferred to internal angular momentum of the fragments during the interaction time [1-3]. The correlations between total kinetic energy and proton number of the projectile-like fragments shown in Fig. 1 for various systems [3] exhibit the large and continuous energy damping down to and below the Coulomb barrier for spherical fragments with an increasing amount of nucleon transfer. In addition, the measurement of γ-ray multiplicities from the deexciting fragments or angular correlations of fragments from fissioning reaction products [4] have recently demonstrated the importance of the transfer of relative angular momentum to intrinsic angular momentum of the fragments. An example for the correlation of measured γ-ray multiplicities with energy loss [3] is shown in Fig. 2. With increasing energy relaxation also the internal angular momentum of the fragments increases and saturates in the completely damped region.

For these heavy systems, the wave length in the relative motion is small as compared to characteristic lengths of the interaction potential. Consequently it is frequently possible to consider collisions between heavy nuclei in the classical limit. According to the classical picture [5] of Figs. 3,4, deeply inelastic collisions occur for impact parameters b

(or relative angular momenta ℓ) sufficiently smaller than the grazing value $b_{gr}(\ell_{gr})$ and larger than the critical value $b_{cr}(\ell_{cr})$ below which the nuclei fuse to from a compound nucleus. In a deeply inelastic collision, the two ions form a rotating composite (dinuclear, binary, two-body) system for an interaction time of the order of 10^{-21}s. Depending on the incident energy and the size of the system, the orbits may be pulled to negative scattering angles by the attractive nuclear potential, but the memory of the entrance channel is not lost completely as in the formation of a compound nucleus. As indicated schematically in Fig. 4, the deeply inelastic collision process is the dominant part of the total reaction cross section for sufficiently heavy systems at incident energies just above the Coulomb barrier up to about 10-20 MeV/A. Beyond this energy, the beam momentum per nucleon becomes larger than the Fermi momentum and consequently equilibration processes between the nuclei become increasingly unimportant [6].

At present various theoretical approaches deal with different aspects of the deeply inelastic collisions. Many studies of the relative motion have been performed by introducing dissipative terms (friction forces) into the classical equations of motion [7]. This allows to calculate gross angular distributions in the classical approximation as well as the mean energy and angular momentum loss. However, no attention is paid to the mass transfer, and the neglect of statistical and quantal fluctuations prevents a complete description of the physical situation. It has been shown by

Nörenberg [8] that the relaxation processes encountered in these reactions can be understood as transport phenomena and described by master equations and Fokker-Planck equations. These equations have also been used by Moretto et al. [1,9], Ngô et al. [10] and others to investigate mass transfer and energy dissipation in deeply inelastic collisions. This approach is complementary to the classical dynamical calculations since the internal degrees of freedom are considered explicitly whereas the relative motion is eliminated. Although very recently several statistical treatments have been developed which explicitly include the relative motion [11], the success of the simple statistical models in particular to describe the mass transfer [8,9,12] justifies a further pursuit of this approach. We subsequently describe the basic equations and the extension of a microscopic quantum-statistical model [13,14] for the calculation of mass and energy transport coefficients to include the angular momentum dissipation [15]. Analytic expressions for mass, energy and angular momentum drift and diffusion coefficients are given. In section 3, we present a phenomenological model to treat the relative motion that allows to determine ℓ-dependent mean interaction times from experimental data [12]. This is used to determine experimental transport coefficients which are compared with the theoretical values to test the validity of the microscopic theory. Alternatively, we can calculate mass or element distributions (section 4) and angular momentum distributions (section 5). Both are compared in detail with recent measurements.

2. Microscopic Transport Theory

Because of the large level densities of the highly excited fragments in deeply inelastic collisions, only mean quantities averaged over many channels are observed. In microscopic transport theories one attempts an accurate treatment of these macroscopic observables which are obtained as averages over internal states in a coarse-graining procedure [16]. For the time evolution of the macroscopic probability distribution $P(\vec{y}, \vec{r}, \vec{p}; t)$ a generalized master equation [5] can be derived. Typical examples for the relevant macroscopic variables $\vec{y} = (y_1, \ldots, y_f)$ are mass asymmetry A_1/A, internal angular momentum component M and total excitation energy E^*. Most of the microscopic transport equations introduced so far [11] treat the relative motion in the classical approximation, i.e. the probability distributions are regarded as narrow distributions in $\vec{r}$ and $\vec{p}$ centered around the mean values. Assuming that the characteristic times in $P(\vec{y}, \vec{r}, \vec{p}; t)$ are large as compared to the memory time [16] which limits the phase coherence in the system, memory effects can be neglected. As discussed by Nörenberg in [5], the generalized master equation then transforms into two coupled equations (2.1) and (2.3). The classical equation of motion for the mean values $\langle \vec{p}(t) \rangle$ is

$$\frac{\partial}{\partial t} \langle \vec{p}(t) \rangle = - \vec{\nabla}_r \langle V \rangle_t - \overleftrightarrow{\gamma}(t) \langle \vec{p}(t) \rangle . \quad (2.1)$$

The mean potential $\langle V \rangle_t$ and the friction tensor $\overleftrightarrow{\gamma}$ are determined by the time-dependent occupation probabilities

$$P(\vec{y},t) = \int d^3r\, d^3p\; \mathcal{P}(\vec{y},\vec{r},\vec{p};t) \tag{2.2}$$

which are solutions of the master equation

$$\frac{\partial}{\partial t} P(\vec{y},t) = \int d^f y'\, w(\vec{y},\vec{y}';t)\left[\varrho(\vec{y})P(\vec{y}',t) - \varrho(\vec{y}')P(\vec{y},t)\right] \tag{2.3}$$

with the level densities ϱ and the transition probability w. In dynamical calculations to describe the relative motion [7], (2.1) is solved usually with phenomenological friction coefficients and potentials. Whereas the simultaneous solution of (2.1) and (2.3) would provide a rather complete description of deeply inelastic collisions, we focus on the treatment of time-irreversible relaxation processes in the macroscopic variables $\vec{y}$ as described by the master equation (2.3). Since matrix elements for one-particle transfer are much larger than for two-particle transfer, the transition probability $w(\vec{y},\vec{y}';t)$ has a width of two mass units only. The width in energy can be estimated [5] as $\Delta \approx 2$ MeV, in angular momentum [15] as $\Delta j \approx 2$. Consequently, the transition probability is essentially different from zero only for $\vec{y} \approx \vec{y}'$ and we may expand $\varrho(\vec{y}')$ and $P(\vec{y}',t)$ around $\vec{y}' = \vec{y}$ in (2.3). Retaining terms up to second order, the Fokker-Planck equation [8] is obtained

$$\frac{\partial P(\vec{y},t)}{\partial t} = -\sum_{i=1}^{f} \frac{\partial}{\partial y_i}\left[v_i(\vec{y},t)P(\vec{y},t)\right] + \sum_{i,j=1}^{f} \frac{\partial^2}{\partial y_i\, \partial y_j}\left[D_{ij}(\vec{y},t)P(\vec{y},t)\right] \tag{2.4}$$

The probability distributions are determined in terms of the drift vector $\vec{v} = (v_1, \ldots, v_f)$ and the diffusion tensor $\{D_{ij}\}$.

The components of the diffusion tensor are defined on the microscopic level [13-16]

$$D_{ij}(\vec{y}) = \tau_{mem}(\vec{y}) \cdot \frac{1}{3} \left\langle \left[\hat{y}_i, \left[\hat{y}_j, V \right] \right] V^+ \right\rangle_{\vec{y}} \qquad (2.5)$$

with the interaction V and the memory time ($\hbar \equiv 1$)

$$\tau_{mem}(\vec{y}) = \left[\pi / \langle V V^+ \rangle_{\vec{y}} \right]^{1/2} . \qquad (2.6)$$

Here the brackets $\langle \ldots \rangle_{\vec{y}}$ denote the mean values over states of the composite system with fixed $\vec{y}$ and $\hat{y}_i$ is the operator corresponding to the variable y_i. The components of the drift vector

$$v_i(\vec{y}) = \frac{1}{\rho(\vec{y})} \sum_{j=1}^{f} \frac{\partial}{\partial y_j} \left[\rho(\vec{y}) D_{ij}(\vec{y}) \right] \qquad (2.7)$$

are determined by the diffusion coefficients and the level density of the composite system. These expressions allow for a microscopic calculation of the transport coefficients. The results of such a calculation may be compared with experimental values of the drift and diffusion coefficients deduced from a comparison between experimental data and the solutions of (2.4) for simplified assumptions about $\vec{v}$ and $\{D_{ij}\}$ [5,8,12,14]. In the following we briefly describe the microscopic model of Ayik et al. [13-15] for the evaluation of (2.5) and (2.7) and give the analytical results.

The macroscopic variables treated explicitly are $\vec{y} = (A_1, M, E^*)$. We evaluate the transport coefficients for these variables in a single-particle model illustrated

schematically in Fig. 5. The mean values in (2.5) and (2.7) are replaced by mean values over simple shell model states of the separated spherical fragments with constant single-particle density. The initial or final state may correspond to the same nucleus (excitation) or to different nuclei (transfer and excitation). Thus, the Hamiltonian can be written as

$$H = H_0 + \sum_{\nu \neq \mu} u_{\nu\mu}\, a_\nu^+ a_\mu \qquad (2.8)$$

with creation and destruction operators a_ν^+, a_μ in single-particle states ν, μ, respectively. Here,

$$H_0 \equiv H_0(A_1, \ell, H) = \sum_\nu \varepsilon_\nu a_\nu^+ a_\nu + U_{\ell H}(A_1) \qquad (2.9)$$

contains the ground state energy $U_{\ell H}(A_1)$ of the composite systems with asymmetry A_1/A, relative angular momentum ℓ and internal angular momentum component M. It is referred to as the driving potential since the mass drift coefficient v_A turns out to be proportional to $\partial U_{\ell H} / \partial A_1$. It is given by

$$U_{\ell H}(A_1) = U(A_1) + \frac{(\ell - H)^2}{2\mathcal{J}_{rel}} + \frac{H^2}{2\mathcal{J}_{int}} \qquad (2.10)$$

$$U(A_1) = U_{LD}(A_1) + U_{LD}(A_2) - U_{LD}(A) + V_C(A_1) + V_N(A_1) \qquad (2.11)$$

with the liquid drop energies U_{LD} (shell effects are neglected), the Coulomb interaction V_C, the nuclear attraction V_N and the relative momentum of inertia $\mathcal{J}_{rel}$ (units MeV^{-1}). The

intrinsic moment of inertia is given within the model as

$$\mathcal{J}_{int} = \frac{1}{6\sqrt{2}} \left(g_1 \bar{j}_1^{-2} + g_2 \bar{j}_2^{-2} \right) \qquad (2.12)$$

with the single-particle level densities $g_k = A_k/12$ MeV^{-1}. We estimate the maximum single-particle angular momentum of fragment $\bar{j}_k$ from the observed shell structure as

$$\bar{j}_k \approx 0.44\, A_k^{1/2}. \qquad (2.13)$$

The matrix elements of the interaction (2.8) are parametrized by a product of Gaussians in the differences of the single-particle energies $(\varepsilon_\nu - \varepsilon_\mu)$, angular momenta $(j_\nu - j_\mu)$ and angular momentum projections $(m_\nu - m_\mu)$ for excitation, or $(m_\nu + m_\mu - \Delta m)$ for transfer, respectively. Four universal parameters enter this expression, an interaction strength factor v, a width Δ given by the mean change of excitation energy in a single step, a corresponding width Δj given by the mean change in angular momentum, and the mean recoil angular momentum Δm arising in particle transfer. Using the method of spectral distributions [17] the mean values in (2.5), (2.6) can be calculated. The components of the diffusion tensor

$$D_{ij}\,(A_1, M, E^*) = \begin{pmatrix} D_{AA} & D_{AM} & 0 \\ D_{MA} & D_{MM} & 0 \\ 0 & 0 & D_{EE} \end{pmatrix} \qquad (2.14)$$

are obtained as

$$D_{AA} = 0.21\,\tilde{\gamma}\,\tilde{\Delta}^{1/2}\left[E^{*}_{eH}(A_1)/A\right]^{1/4}\left[\frac{(A_1A_2)^{1/3}}{A_1^{1/3}+A_2^{1/3}}\right]^2 \qquad (2.15)$$

$$D_{HH} = \frac{(\Delta J)^2}{(\Delta J)^2+0.033A}\left[D_{AA}\cdot 0.002\,A_1A_2/(\Delta J)^2 + D_{EE}\cdot 0.033A/\tilde{\Delta}^2\right] + D_{AH}^2/D_{AA} \qquad (2.16)$$

$$D_{EE} = 0.053\,\tilde{\gamma}\,\tilde{\Delta}^{5/3}\left[E^{*}_{eH}(A_1)/A\right]^{1/4}(A_1A_2)^{1/3} \qquad (2.17)$$

$$D_{AH} = D_{HA} = D_{AA}\cdot(\Delta m)\cdot\frac{0.033(A_1-A_2)}{(\Delta J)^2+0.033A} \qquad (2.18)$$

$$D_{EA} = D_{EH} = 0 \qquad (2.19)$$

with

$$\tilde{\Delta} = \Delta\left[1+\frac{\Delta^2 A}{32\,E^{*}_{eH}(A_1)}\right] \qquad (2.20)$$

$$\tilde{\gamma} = \gamma\left[\frac{(\Delta J)^2}{(\Delta J)^2+0.033A}\right]. \qquad (2.21)$$

The units of the diffusion coefficients are $10^{22}s^{-1}$ except for D_{EE} which is in $10^{22}MeV^2s^{-1}$. As indicated in Fig. 6, the local excitation energy $E^{*}_{eH}(A_1)$ is related to the excitation energy E^{*} for symmetric fragmentation with $e=H=0$ (which is an independent variable) via

$$E^{*}_{eH}(A_1) = E^{*} - U(A_1) + U(A/2) - \frac{(e-H)^2}{2\mathcal{J}_{rel}} \qquad (2.22)$$

The diffusion coefficients depend only weakly on e and H

according to

$$\mathcal{D}_{ij}(\ell,M) \propto \left[E^{*}_{\ell M}(A_1)\right]^{1/4} . \qquad (2.23)$$

For large relative angular momenta $\ell \geq \ell_{max}$, however, an additional form factor $\rho(\ell)$ has to be taken into account since the diffusion is not fully developed. We use a parametrization which is in good agreement with an analysis of experimental data [12]

$$\rho(\ell) = \begin{cases} 1 , & \ell < \ell_f \\ (\ell_{gr} - \ell)/(\ell_{gr} - \ell_f) , & \ell_f \leq \ell \leq \ell_{gr} . \end{cases} \qquad (2.24)$$

Here, ℓ_f is taken as the angular momentum on a Coulomb trajectory with the minimal distance equal to the close contact radius $R_0 = 1.2\,(A_1^{1/3} + A_2^{1/3})$.

The mixed coefficient $\mathcal{D}_{AM}$ describes the coupling between mass and angular momentum transfer due to the recoil. It is generally small compared to $\mathcal{D}_{MM}$ and $\mathcal{D}_{AA}$ and vanishes completely for transfers between equal fragments because here the recoil effect is averaged out.

For the drift coefficients (2.7) we obtain [15]

$$v_A = -\frac{1}{T_{\ell M}}\left[\mathcal{D}_{AA}\frac{\partial U_{\ell M}(A_1)}{\partial A_1} + \mathcal{D}_{AM}\left(\frac{M}{\mathcal{J}_{int}} - \frac{\ell - M}{\mathcal{J}_{rel}}\right)\right] \qquad (2.25)$$

$$v_M = -\frac{1}{T_{\ell M}}\left[\mathcal{D}_{MM}\left(\frac{M}{\mathcal{J}_{int}} - \frac{\ell - M}{\mathcal{J}_{rel}}\right) + \mathcal{D}_{AM}\frac{\partial U_{\ell M}(A_1)}{\partial A_1}\right] . \qquad (2.26)$$

$$v_E = \frac{1}{T_{eH}} D_{EE} \tag{2.27}$$

with the temperature (in MeV)

$$T_{eH}(A_1) = 3.46 \left[E^*_{eH}(A_1)/A \right]^{1/2}. \tag{2.28}$$

In the "sticking limit"

$$M \to M_{st} = \frac{\mathcal{J}_{int}}{\mathcal{J}_{int} + \mathcal{J}_{rel}} \ell \tag{2.29}$$

the angular momentum drift coefficient v_H practically vanishes since the second term is a small contribution. This limit which is familiar from classical mechanics appears in the microscopic calculation due to the spin cut-off factor in the level densities. As long as it is not reached, both terms in (2.25) contribute to the mass drift, partially cancelling each other. Once sticking is attained, the second term vanishes, and the mass drift coefficient is proportional to $\partial U_{rot}/\partial A_1$. The mass drift coefficient has a rather strong dependence on the relative angular momentum ℓ. In the sticking limit, this reflects the ℓ-dependence of the driving potential. The dependence of mass and energy transport coefficients on mass asymmetry A_1/A, total mass A and relative angular momentum ℓ have been investigated in detail in [14].

In phenomenological applications of the Fokker-Planck equation (2.4) to a system with given A, usually constant mass transport coefficients have been assumed [8,12,18]. According to the theoretical expressions, this assumption

may be justified for mass fragmentations A_1/A sufficiently far from symmetry ($A_1 = A_S \equiv A/2$) and relative angular momenta ℓ not too much different from a mean $\bar{\ell}$. In general, however, the ℓ-dependence of v_A must be taken into account when comparing solutions of the Fokker-Planck equation and experimental mass distributions. For systems with the projectile mass A_P close to the symmetric value ($A_P = A_S$), also the dependence of v_A on mass asymmetry A_1/A has to be considered. A linear approximation of v_A close to symmetry is sufficiently accurate, allowing for an analytical solution of the Fokker-Planck equation. Note that the mass drift vanishes for $A_1 = A_S$.

The dependences of the angular momentum transport coefficients on intrinsic angular momentum M/M_{st}, mass asymmetry A_1/A and total mass A are shown in Fig. 7 for several values of the initial relative angular momentum ℓ/ℓ_{gr} and fixed total excitation energy E^*/A = 1 MeV. Here, the grazing angular momentum

$$\ell_{gr} = 0.22\, R \left[A_{red} \left(E - V_c(R) \right) \right]^{1/2} \qquad (2.30)$$

with $A_{red} = A_1 A_2 / A$ is determined by the interaction radius $R = 0.5 + 1.36\,(A_1^{1/3} + A_2^{1/3})$ and the center-of-mass energy E. The drift coefficient depends almost linearly on intrinsic angular momentum M and vanishes as the sticking limit ($M/M_{st} = 1$) is reached, whereas the diffusion coefficient remains nearly constant. This will allow us to calculate analytically mean value and variance of the internal angular momentum distributions, cf. section 5.

In the explicit calculation of the transport coefficients, the values of the model parameters Δ, γ, ΔJ and Δm have to be fixed. We estimate $\Delta J \approx 2$ from the uncertainty of the transferred momentum due to the size of the window. The recoil angular momentum can be estimated as $\Delta m \approx \ell/(2A_{recl})$ with typical values $\Delta m \leq 2$. Since the influence of the mixed diffusion coefficient is generally small, we neglect the ℓ-dependence and take $\Delta m = 1$. The product $\tilde{\gamma}\tilde{\Delta}^{1/2} = 2.2$ MeV$^{1/2}$ (cf. (2.26), (2.24)) has been determined in a fit [12] to the experimental mass diffusion coefficient in the reaction ^{84}Kr(714 MeV) + ^{165}Ho. This is fulfilled for $\Delta = 2$ MeV and $\gamma = 3$, corresponding to reasonable values of the interaction strength parameter γ and the width Δ. The transport coefficients are usually evaluated at the close contact radius $R_0 = 1.2\ (A_1^{1/3} + A_2^{1/3})$. With these choices, the values of the theoretical transport coefficients are determined and they may be used to calculate cross sections, or compared to experimental values (sections 4,5).

3. Mean Interaction Time

On the basis of the Fokker-Planck equation (2.4), experimental drift and diffusion coefficients can be determined from measured cross sections, or cross sections may be calculated using the theoretical transport coefficients provided the mean interaction time $\tau_{i,\ell}$ is known. Whereas the nuclear contact time can be obtained in solutions [7] of the classical equation of motion (2.1), it is often preferred to determine it from experimental data [8,12,18,19,20]. Rough estimates of $\tau_{i,\ell}$ [8] turn out to be too crude and lead to considerable errors in the deduced values of experimental transport coefficients. We subsequently describe a method [12] which seems appropriate to obtain the mean interaction time rather accurately from experimental information. It relies on the determination of a parametrized mean deflection function $\Theta(\ell)$ from the measured angular distribution and takes into account the mean energy and angular momentum loss.

The classical model underlying the determination of $\tau_{i,\ell}$ as function of ℓ (or b) is outlined in Fig. 8. The angle of rotation of the composite system during nuclear contact is

$$\Delta\vartheta = \pi - \vartheta_i - \vartheta_f - \Theta \qquad (3.1)$$

The construction of the deflection function from the experimental angular distribution will be described below. The respective Coulomb angles ϑ_i, ϑ_f in entrance and exit channel depend on radius, energy and angular momentum

$$\vartheta_i = \vartheta(R, E, \ell)$$
$$\vartheta_f = \vartheta(R_f, E_f, \ell_f) . \qquad (3.2)$$

They can be written as

$$\vartheta = \arcsin \frac{2b/R + \varepsilon}{\sqrt{4+\varepsilon^2}} - \arcsin \frac{1}{\sqrt{(2\varepsilon)^2+1}} \qquad (3.3)$$

with $\varepsilon = Z_1 Z_2 e^2/(\epsilon b)$ and $b = \ell/\sqrt{2\mu E}$. Note that $\pi - \vartheta_i - \vartheta_f$ is not equal to the Rutherford deflection angle as has been assumed in [19] , the difference being typically a factor 1.5-2. Neglecting deformations, we take the scission radius to be $R_f = R$. In the sticking limit, the mean exit channel relative angular momentum is given by

$$\ell_f = \ell_{st} = \frac{\mathcal{J}_{rel}}{\mathcal{J}_{rel} + \mathcal{J}_{int}^{cl}} \ell \qquad (3.4)$$

with the relative moment of inertia $\mathcal{J}_{rel} = \mu R_c^2$ and the intrinsic moment of inertia which is assumed here to have the classical value $\mathcal{J}_{int}^{cl} = \frac{2}{5} m_1 R_1^2 + \frac{2}{5} m_2 R_2^2$. The interaction time becomes in this limit ($\mathcal{J}_{tot} = \mathcal{J}_{rel} + \mathcal{J}_{int}^{cl}$)

$$\tau_{st} = \Delta\vartheta \cdot \mathcal{J}_{tot} / \ell . \qquad (3.5)$$

The gradual dissipation of angular momentum is taken into account according to the following parametrization

$$\ell_f(\ell) = \ell_{st} + (\ell - \ell_{st}) e^{-\omega \tau_{st}} \qquad (3.6)$$

This expression is almost identical to a result derived in the statistical theory (cf. (5.3)). The difference is that the theoretical angular momentum relaxation constant is weakly ℓ-dependent whereas here we use a constant μ and the time in the exponential is approximated by τ_{sl} in order to be able to derive an analytical expression for the mean interaction time. The resulting equation

$$\tau_{int}(\ell) = \frac{\Delta\vartheta \cdot J_{tot}}{\ell} + \frac{1}{\mu} \ln\left(\frac{\ell_f}{\ell_i}\right) \qquad (3.7)$$

is solved by iteration taking $\ell_f = \ell_{if}$ for the calculation of $\Delta\vartheta$ in the first step. We determine both μ and the exit channel energy $\bar{E}_f$ needed for the calculation of the Coulomb angle ϑ_f from the experimental energy loss. Under the assumption that the radial energy is completely dissipated during the interaction time, $\bar{E}_f$ can be written as

$$E_f = \frac{Z_1 Z_2 e^2}{R} + \frac{\ell_f^2}{2\mu R^2} \qquad (3.8)$$

As shown in Fig. 9, this allows to fit the mean experimental energy loss for those values of the initial relative angular momentum ℓ (or the interaction time $\tau_{int}(\ell)$) where deformations are not important and determines simultaneously $\bar{E}_f$ and ℓ_f. For the reaction ^{84}Kr (714 MeV) + ^{165}Ho we have obtained a value $1/\mu = 1.5 \cdot 10^{-21}$ s [12] which is also used to calculate the mean interaction times for the systems investigated in sections 4,5. The form factor (2.24) is included in the calculation.

For obtaining the mean deflection function $\Theta(\ell)$ or $\Theta(b)$ from the measured angular distribution (integrated over all fragments and energies) we use the parametrization

$$\Theta(b) = \Theta_C(b) + \Theta_N(b) . \tag{3.9}$$

At large impact parameters the scattering angle is given by the Coulomb deflection function

$$\Theta_C(b) = 2\arctan \frac{Z_P Z_T e^2}{2Eb} \tag{3.10}$$

The "nuclear part" Θ_N is taken of the form

$$\Theta_N(b) = -\beta\, \Theta_C^{gr} \frac{b}{b_{gr}} \left(\frac{\alpha}{\beta}\right)^{b/b_{gr}} \tag{3.11}$$

with the Coulomb deflection angle Θ_C^{gr} on the grazing trajectory and the grazing impact parameter usually being determined from a quarter-point analysis of elastic scattering data. The parameters β and α are adjusted to fit the angular distribution which is calculated in the classical approximation

$$\frac{d\sigma}{d\Theta} = 2\pi \sum_n b_n \left|\frac{db}{d\Theta}\right|_{b=b_n} \tag{3.12}$$

An example for the determination of the deflection function [12] is shown in Fig. 10 for the Kr + Ho reaction. Since we are interested only in the mean interaction time we do not consider the quantal and statistical fluctuations which smooth out the angular distributions, giving a better agreement with the data. The decomposition of the experimental cross

section into a positive and a negative angle part has been described in [21]. Negative angle scattering is encountered in reactions with values of $\eta' = Z_P Z_T e^2/\hbar v' \leq 200$ for a modified Sommerfeld parameter η' where $v' = [2/\mu (E - V_c(R))]^{1/2}$ is the relative velocity at the interaction radius R. This phenomenological parameter which has been introduced by Galin [1] seems to allow for a classification of deeply inelastic heavy ion reactions according to their angular distributions [22].

From the reactions investigated so far, it appears that both parameters β and α in the deflection function are monotonic functions of η'. Note that η' reflects the balance of Coulomb and friction forces at the interaction radius. For low energies, or large values of η' the rotating system does not reach negative angles and the deflection function has a nuclear rainbow in the positive angle region. This can be seen in Fig. 11 for the reactions ^{86}Kr (515 MeV) + ^{166}Er and ^{132}Xe (779 MeV) + ^{120}Sn. The deflection functions as deduced in [23] from the data of Gobbi et al. [3] and the calculated interaction times are shown. Apart from a form factor close to ℓ_{gr} the times increase exponentially with decreasing ℓ. They are in rather good agreement with the results of a recent dynamical calculation [24].

For even heavier systems with very large values of η such as the ^{238}U (1766 MeV) + ^{238}U reaction the deflection function deduced from the data of Hildenbrand et al. [25] becomes Coulomb-like and the corresponding angle of rotation is rather small. On the other hand, the moment of inertia

is very large, and consequently the interaction time (3.7) for this system is larger than in the other reactions for high ℓ, but smaller in the low-ℓ region. It should be kept in mind, however, that the effect of deformations on the mean interaction time has been neglected in (3.7), causing a possibly large uncertainty in the U+U reaction.

4. Mass Transport

The mean interaction times obtained in the previous section can be used to calculate cross sections with the theoretical transport coefficients of section 2. As an example, we calculate element distributions which are compared with the data for the reactions considered in section 3. For simplicity we neglect the coupling between mass and angular momentum transport. The mass diffusion coefficients are assumed to be constant, and the theoretical values (2.15) are calculated for the initial fragmentation and a mean $\bar{\epsilon}$. Complete energy relaxation and $M = M_{st}$ is assumed to obtain $E^{*}_{\varrho M}(A_1)$. For the Kr + Ho and the Kr + Er reactions the initial fragmentation is far from symmetry and we take also the mass drift coefficients as constants. To obtain element rather than mass distributions we convert to charge transport coefficients

$$D_z = \left(\frac{Z}{A}\right)^2 D_{AA} \tag{4.1}$$

$$v_z = \left(\frac{Z}{A}\right) v_A \tag{4.2}$$

This implies equal charge densities, or the assumption of a rapid equilibration of the charge densities which seems rather well fulfilled in deeply inelastic collisions [1]. The Fokker-Planck equation (2.4) then describes the mass transport measured by the proton number. The solution is a Gaussian [8]

$$P(Z_1, t) = (4\pi D_z t)^{-1/2} \exp\left[-\frac{(Z_1 - Z_p - v_z t)^2}{4 D_z t}\right] \tag{4.3}$$

with mean value

$$\langle Z_1 \rangle = v_2 t \tag{4.4}$$

and variance

$$\sigma_2^2 = \langle (Z_1 - \langle Z_1 \rangle)^2 \rangle = 2 D_2 t \tag{4.5}$$

increasing linearly in time. The observed element distributions correspond to the solution (4.3) for $t = \tau_{int}(\theta)$. For weakly focussed reactions such as 8.5 MeV/A Kr+Ho or Ar+Th [8], time and angle are uniquely related, and (4.4), (4.5) may directly be compared to the experimental element distributions at different scattering angles θ, and experimental transport coefficients can be deduced [8,12]. In reactions which do not exhibit a monotonic relation $\tau_{int}(\theta)$ such as 5.99 MeV/A Kr+Er this is not possible, but we can calculate the energy and angle integrated element distribution

$$\left(\frac{d\sigma}{dZ_1}\right)_{DIC} = \frac{2\pi}{k^2} \int_{\ell_{cr}}^{\ell_{max}} \ell \, P\left[Z_1, \tau_{int}(\ell)\right] d\ell . \tag{4.6}$$

The maximum angular momentum ℓ_{max} is determined from the requirement that the total cross section for deeply inelastic events

$$\sigma_{DIC} = \int \left(\frac{d\sigma}{dZ_1}\right)_{DIC} dZ_1 \tag{4.7}$$

agrees with the experimental value. For the Xe + Sn and the

U + U reaction, the initial fragmentation is close to, or agrees with the symmetric mass split, and the linear dependence of v_z on Z_1 has to be taken into account

$$v_z = a\,(1 - b\,Z_1/Z)\,. \tag{4.8}$$

The Fokker-Planck equation can still be solved analytically with the result

$$P(Z_1,t) = \left[\frac{2\pi D_2 \cdot Z}{ab}\left(1 - e^{-2abt/Z}\right)\right]^{-1/2} \exp\left\{ - \frac{\left[Z_1 - Z_0 + \left(Z_p - \frac{1}{b}Z\right)\left(1 - e^{-abt/Z}\right)\right]^2}{\frac{2D_2 \cdot Z}{ab}\left(1 - e^{-2abt/Z}\right)} \right\}. \tag{4.9}$$

Here, b = 2. Again the element distributions are calculated according to (4.6). The results [23] for the reactions Kr + Er, Xe + Sn and U + U are summarized in Fig. 12. We show several normalized solutions $P(Z_1,t)$ of the Fokker-Planck equation to illustrate mass drift and diffusion as functions of time. The asymmetric Kr + Er system exhibits a sizable drift towards symmetry. The theoretical calculation of the element distribution as shown by the dashed curve is in rather good agreement with the data [3]. Since the interaction time is determined by the procedure outlined in section 3, and the parameters in the theoretical transport coefficients (section 2) have been fixed [12], there is little room for an improvement of this calculation within the framework used here. Taking the ϑ-dependence of the transport coefficients (in particular, of the drift coefficient) into account rather than using a mean $\bar{\vartheta}$ may further improve the agreement, and in addition one has to consider that the

experimental data have not yet been corrected for the emission of charged particles. The solid curve is obtained by adjusting the drift coefficient to fit the data. The corresponding experimental results for the transport coefficients are shown in Table 1 together with the theoretical values.

The Xe + Sn system is nearly symmetric and the solution (4.9) of the Fokker-Planck equation is used to calculate the element distribution. The attempt to improve the result of the calculation (dashed curve) by adjusting the transport coefficients (solid curve) is not very successful. The reason seems to be that the data exhibit a drift towards the closed proton shell $Z_1 = 50$ superimposed on the drift towards symmetry $(Z_1 = Z_2 = 52)$ which is included in the approach used here. The additional treatment of shell effects is presently investigated by Schürmann et al. [26]

In the U + U reaction, most of the deeply inelastic cross section undergoes sequential fission. The experimental cross section [25] is given by the black squares in Fig. 12. The result of an attempt to reconstruct the primary deeply inelastic element distribution prior to fission is shown by the open squares [25]. Corrections for charged particle emission have not been made. The calculation (dashed curve) fails to reproduce the reconstructed element distribution. The diffusion coefficient extracted from a fit to this distribution is larger than the theoretical value by more than a factor of 2 (Table 1). Although the neglect of deformations in the calculation of the mean interaction time may have a severe effect in the U + U case, it seems too early to draw decisive conclusions from this disagreement.

5. Angular Momentum Dissipation

The theoretical angular momentum drift and diffusion coefficients of section 2 can be used to calculate mean value $\langle H \rangle$ and variance σ_H^2 of the internal angular momentum distribution of both fragments as functions of time. Again we neglect the coupling between angular momentum and mass transport. In section 2, the linear dependence of the drift coefficient v_H on the z-component of the internal angular momentum, and the H-independence of the diffusion coefficient has been discussed (cf. Fig.7). Using this information together with the Fokker-Planck equation for the variable H, we have

$$\frac{d}{dt}\langle H \rangle = v_H(H=0) + \langle H \rangle \left.\frac{\partial v_H}{\partial H}\right|_{H=0} \tag{5.1}$$

and

$$\frac{d}{dt}\sigma_H^2 = 2D_{HH}(H=0) + 2\sigma_H^2 \left.\frac{\partial v_H}{\partial H}\right|_{H=0} \tag{5.2}$$

Integration of (5.1), (5.2) yields mean value and variance of the angular momentum distribution

$$\langle H \rangle = H_{st}\left(1 - e^{-\omega_e t}\right) . \tag{5.3}$$

$$\sigma_H^2 = \frac{D_{HH}}{\omega_e}\left(1 - e^{-2\omega_e t}\right) . \tag{5.4}$$

The relaxation constant is given by

$$\omega_e = \frac{D_{HH}}{T_{eH}} \left.\frac{\mathcal{J}_{in} + \mathcal{J}_{out}}{\mathcal{J}_{in} \cdot \mathcal{J}_{out}}\right|_{H=0} . \tag{5.5}$$

It is only weakly ℓ-dependent. For large times, the mean value of the intrinsic angular momentum approaches the sticking limit, whereas the variance reaches a saturation value $\mathcal{D}_{HH}/\mu\ell_c$.

With the mean interaction time $t = \tau_{int}(\ell)$ as determined in section 3, we can evaluate (5.3), (5.4) as functions of τ_{int} or ℓ . As an example, we show the results for the Kr + Er reaction in Fig. 13. The mean value reaches the sticking limit for $\ell \lesssim 100$, whereas the variance saturates in the low-ℓ region.

From γ- multiplicity measurements [4], the mean absolute angular momentum I_{tot} of both fragments with angular momenta $\vec{I}_1$, $\vec{I}_2$ is obtained

$$I_{tot} = \langle I_1^2 \rangle^{1/2} + \langle I_2^2 \rangle^{1/2} . \qquad (5.6)$$

This is equal to, or larger than the mean internal angular momentum of the composite system [15]

$$\langle I^2 \rangle^{1/2} = \langle (\vec{I}_1 + \vec{I}_2)^2 \rangle^{1/2} \leq I_{tot} . \qquad (5.7)$$

Although we have considered so far only the z-component M of the internal angular momentum of the composite system, $\langle I^2 \rangle^{1/2}$ can be estimated. Since the recoil angular momentum is parallel to the z- direction, we expect that the mean value of the internal angular momentum in the x- and y- direction is

zero. The variances of the angular momentum components perpendicular to the symmetry (y-) axis are likely to be equal. Because of axial symmetry of the composite system, creation of angular momentum along the symmetry axis is expected to be small. Thus we obtain for the internal angular momentum of both fragments

$$\langle I^2 \rangle^{1/2} = \left[c\,\sigma_H^2 + \langle H \rangle^2 \right]^{1/2} \qquad (5.8)$$

with $2 \leq c \leq 3$. The results for $c = 3$ are shown in Fig.13. We have also plotted data points for I_{tot}^{exp} obtained by Gobbi et al. [27] from the analysis of a γ- multiplicity experiment [3] (cf. Fig. 2) . Since we are presently not able to calculate $\langle I^2 \rangle_{exp}^{1/2}$ from I_{tot}^{exp} , the comparision is for slightly different physical quantities, cf. (5.7). Although the equality in (5.7) is expected to be fulfilled best for sufficiently large values of ℓ [15] , the calculation reproduces the measured saturation in the low-ℓ region reasonably well. It is realized that treatments of the angular momentum dissipation which consider only the mean values (such as classical dynamical calculations with friction forces) will fail to describe the angular momentum transport in the completely damped region.

Finally we have calculted the alignment of the composite system along the z- direction (Fig. 13)

$$P_{zz} \equiv \frac{3}{2} \frac{\langle H^2 \rangle}{\langle I^2 \rangle} - \frac{1}{2} \qquad (5.9)$$

The calculated alignment is large for most of the partial waves, but experimental data are not yet available for comparision.

6. Summary

We have investigated relaxation processes in deeply inelastic collisions between heavy nuclei. The main goal has been to achieve a simple understanding of these processes on the basis of a Fokker-Planck equation. A microscopic model that allows to calculate drift and diffusion coefficients for the macroscopic variables mass asymmetry, z-component of the internal angular momentum and total excitation energy has been discussed, with particular emphasis on the angular momentum transport. The theoretical transport coefficients are functions of total excitation energy, total mass, mass fragmentation, relative and internal angular momentum.

Rather than treating the relative motion by solving the equations of motion, we determine angular momentum dependent mean interaction times from experimental data. In particular, this involves the construction of mean deflection functions from the measured angular distributions. The parametrization of the deflection function used here seems suitable to account for the change in angular distributions encountered in deeply inelastic collisions depending on the incident energy and the size of the system.

With the mean interaction times and the theoretical mass transport coefficients, we have calculated element distributions for asymmetric (Kr + Er, Kr + Ho) as well as for symmetric (Xe + Sn, U + U) systems. The comparison with the experimental data clearly demonstrates the applicability of

our model to the mass transport phenomena. It should be noted, however, that the accurate calculation of double differential cross sections $d^2\sigma/dEdZ_1$ is a much more difficult problem than the calculation of the energy integrated element distributions shown here. In the Xe + Sn reaction, the comparison between calculation and data seems to indicate the presence of shell effects which have not yet been included in the theory. The experimental cross section in the U + U reaction which has been reconstructed from the yields after sequential fission is not reproduced by the calculation. A reason for the disagreement may be an underestimate of the mean interaction time due to the neglect of deformations.

With the theoretical angular momentum transport coefficients we have calculated mean value and variance of the angular momentum distribution. For small values of the initial relative angular momentum ℓ the mean value reaches the sticking limit, whereas the variance saturates. The mean internal angular momentum as function of ℓ is found to be in good agreement with a recent γ-multiplicity experiment.

The energy transport has not been considered explicitly here, although we have given the corresponding theoretical drift and diffusion coefficients. The analysis of the experimental energy loss (Fig. 9) is consistent with the view that the radial energy is completely dissipated during the interaction time. This would imply a rather short

relaxation time ($\lesssim 0.3 \cdot 10^{-21}$s) compared to the angular momentum relaxation time of $1/\ell = 1.5 \cdot 10^{-21}$s or the characteristic time for the development of fragment deformations ($\approx 2 \cdot 10^{-21}$s, cf. Fig. 9). If this turned out to be the correct interpretation of the data, experimental energy distributions would only allow for a test of a lower limit for the energy drift coefficient. During the initial stage of the collision, coherent excitations [28] may be responsible for a large fraction of the kinetic energy loss, whereas the irreversible statistical processes we have been dealing with take over at a later stage of the collision.

The collaboration with S. Ayik and W. Nörenberg is gratefully acknowledged, as well as discussions of the experimental data with S. Björnholm, A. Gobbi and H.J. Specht.

References

1. J. Galin, European Conference on Nuclear Physics with Heavy Ions, Caen (1976), J. Phys. C5 37 (1976) 83;

L.G. Moretto and R. Schmitt, European Conference on Nuclear Physics with Heavy Ions, Caen (1976), J. Phys. C5 37 (1976) 109

2. W.U. Schröder and J.R. Huizenga, to be published in Ann. Rev. Nucl. Sc.

3. A. Gobbi et al., International Meeting on Heavy Ion Collisions, Oak Ridge National Laboratory, Pikeville 1977;

U. Lynen et al., X Masurian Summer School in Nuclear Physics 1977, to be published in Nukleonika

4. R. Albrecht, W. Dünnweber, G. Graw, H. Ho, S.G. Steadman and J.P. Wurm, Phys. Rev. Lett. 34 (1975) 1400;

R. Bock, B. Fischer, A. Gobbi, K. Hildenbrand, W. Kohl, U. Lynen, I. Rode, H. Stelzer, R. Albrecht, B.B. Back, G. Auger, J. Galin, J.M. Lagrange, Proceedings of the European Conference on Nuclear Physics with Heavy Ions, Caen, 1976, p. 167;

M. Berlanger, M.A. Delep lanque, C. Gerschel, F. Hanappe, M. Leblanc, J.F. Mayault, C. Ngô, D. Paya, N. Perrin, J. Péter, B. Tamain and L. Valentin, Proceedings of the European Conference on Nuclear Physics with Heavy Ions, Caen, 1976, p. 173

P. Glässel, R.S. Simon, R.M. Diamond, R.C. Jared, I.Y. Lee, L.G. Moretto, J.O. Newton, R. Schmitt and F.S. Stephens, Phys. Rev. Lett. 38 (1977) 331

P. Dyer, R.J. Puigh, R. Vandenbosch, T.D. Thomas and M.S. Zisman, Phys. Rev. Lett. 39 (1977) 392

5. W. Nörenberg, European Conference on Nuclear Physics with Heavy Ions, Caen (1976), J. Phys. C5 37 (1976) 141

6. M. Buenerd, C.K. Gelbke, B.G. Harvey, D.L. Hendrie, J. Mahoney, A. Menchaca-Rocha, C. Olmer and D.K. Scott, Phys. Rev. Lett. 37 (1976) 1191;

J. Hüfner, C. Sander and G. Wolschin, to be published

7. D.H.E. Gross, H. Kalinowski and J.N. De, in Classical and Quantum-Mechanical Aspects of Heavy-Ion Collisions, ed. by H.L. Harney et al. (Springer-Verlag, Berlin-Heidelberg-New York, 1975);

J.P. Bondorf, J.R. Huizenga, M.I. Sobel and D. Sperber, Phys. Rev. C11 (1975) 1265;

F. Beck, Phys. Lett. 62B (1976) 385;

H.H. Deubler and K. Dietrich, Nucl. Phys. A277 (1977) 493;

K. Siwek-Wilczynska and J. Wilczynski, Nucl. Phys. A264 (1976) 115

8. W. Nörenberg, Phys. Lett. 52B (1974) 289

9. L.G. Moretto and J.S. Sventek, Phys. Lett. 58B,(1975) 26;

J.S. Sventek and L.G. Moretto, Phys. Lett. 65B (1976) 326

10. C. Ngô, J. Péter, P. Tamain, M. Berlanger and F. Hanappe, Nucl. Phys. A267 (1976) 181

11. C.M. Ko, H. Pirner and H.A. Weidenmüller, Phys. Lett. 62B (1976) 248;

D. Agassi, C.M. Ko and H.A. Weidenmüller, Ann. Phys. (N.Y.), in press;

H.A. Weidenmüller, International Meeting on Heavy Ion Collisions, Oak Ridge National Laboratory, Pikeville 1977;

K. Dietrich, Nukleonika 21 (1976) 89;

J.P. Siemens and H. Hofmann, Nucl. Phys. A257 (1976) 165 and A275 (1977) 464;

S. Ayik, Phys. Lett. 63B (1976) 22;

S. Ayik and W. Nörenberg, to be published;

W. Nörenberg, S. Ayik, B. Schürmann and G. Wolschin, to be published

12. G. Wolschin and W. Nörenberg, Z. Physik A, in press

13. S. Ayik, B. Schürmann and W. Nörenberg, Z. Physik A277 (1976) 299

14. S. Ayik, B. Schürmann and W. Nörenberg, Z. Physik A279 (1976) 145

15. S. Ayik, G. Wolschin and W. Nörenberg, Z. Physik A, to be published

16. W. Nörenberg, Z. Physik A274 (1975) 241 and A276 (1976) 84

17. S. Ayik and J.N. Ginocchio, Nucl. Phys. A221 (1974) 285 and A234 (1974) 13

18. J.R. Huizenga, J.R. Birkelund, W.U. Schröder, K.L. Wolf and V.E. Viola,Jr., Phys. Rev. Lett. 37 (1976) 885

19. J.R. Huizenga, Nukleonika 20 (1975) 291

20. W.U. Schröder, J.R. Birkelund, J.R. Huizenga, K.L. Wolf and V.E. Viola,Jr., Phys. Rev. C16 (1977) 623

21. K.L. Wolf and C.T. Roche, in Proc. of the Macroscopic Features of Heavy Ion Collisions, Argonne, April 1976

22. M.Lefort, Contribution to the Symposium on New Avenues in Nuclear Physics, Rehovot 1976;

H.J. Specht, Summer School of the Scottish Universities 1977

23. G. Wolschin, X Masurian School in Nuclear Physics 1977, to be published in Nukleonika

24. F. Beck, J. Blocki, M. Dworzecka and G. Wolschin, to be published

25. K.D. Hildenbrand, H. Freiesleben, F. Pühlhofer, W.F.W. Schneider, R. Bock, D. v.Harrach and H.J. Specht, to be published

26. B. Schürmann, W. Nörenberg and M. Simbel, Z. Physik A, to be published

27. A. Gobbi, private communication

28. R. Broglia, C. Dasso and A. Winther, Phys. Lett. 53B (1974) 301 and 61B (1976) 113

Reaction	E_{lab}/MeV	$\bar{\ell}$	v_A^{th}	v_A^{exp}	D_A^{th}	D_A^{exp}	Ref.
$^{86}Kr + ^{166}Er$	515	147	0.40	0.26	1.89	1.89	[23]
$^{132}Xe + ^{120}Sn$	779	160	-0.06	-0.08	1.98	1.60	[23]
$^{84}Kr + ^{165}Ho$	714	224	0.50		2.40	2.40	[12]
$^{136}Xe + ^{209}Bi$	1130	327	0.50	0.35	2.83	4.0	[11]
$^{238}U + ^{238}U$	1766	342	0	0	3.2	7.5	[23]

Table 1. Experimental and theoretical mass transport coefficients in units of $10^{22}s^{-1}$. The theoretical values are calculated for a mean angular momentum $\bar{\ell}$ and the initial fragmentation.

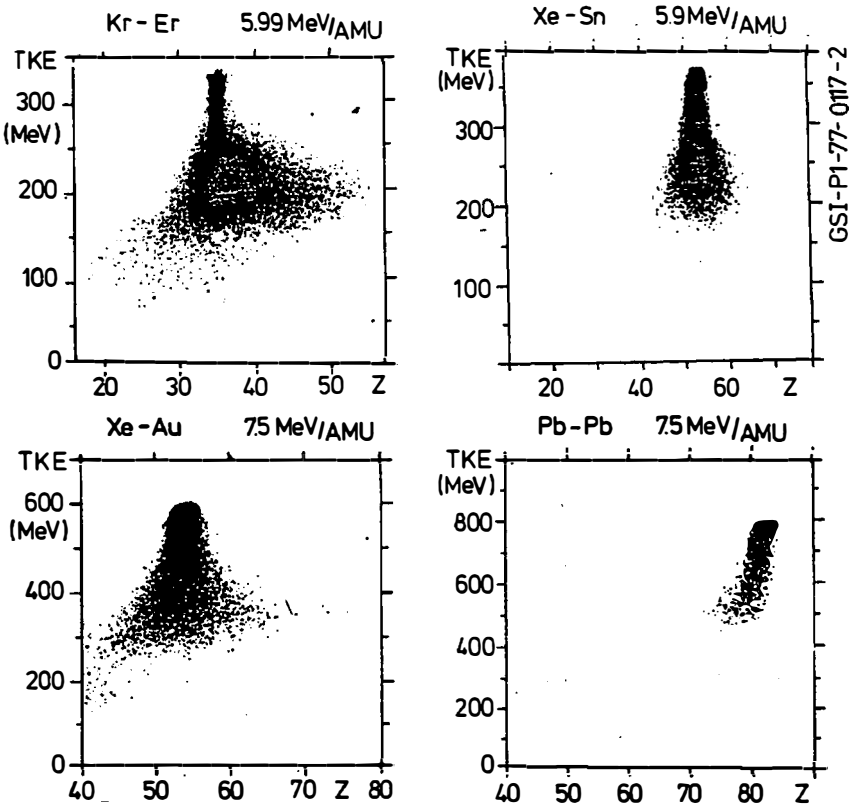

Fig. 1 Measured correlations between total kinetic energy (TKE) and proton number of projectile-like fragments in collisions between heavy nuclei. (From [3]).

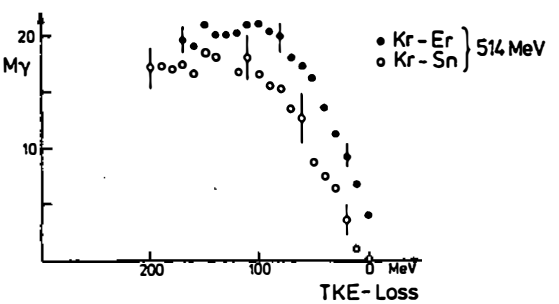

Fig. 2 Measured correlations between γ-multiplicities from deexciting fragments and total kinetic energy loss (From [3]).

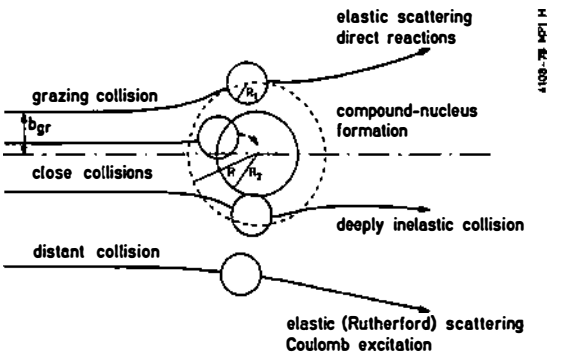

Fig. 3 Classical picture [5] of distant, grazing (quasi-elastic) and close (deeply inelastic, fusion) collisions between heavy nuclei.

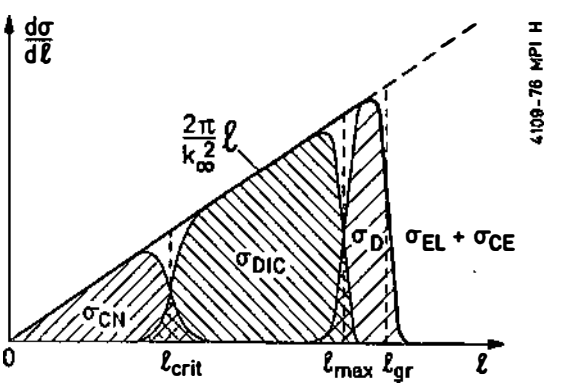

Fig. 4 Decomposition of the total reaction cross section in the cross sections for compound-nucleus formation (σ_{CN}), deeply inelastic collisions (σ_{DIC}) and direct reactions (σ_D). (From [5]).

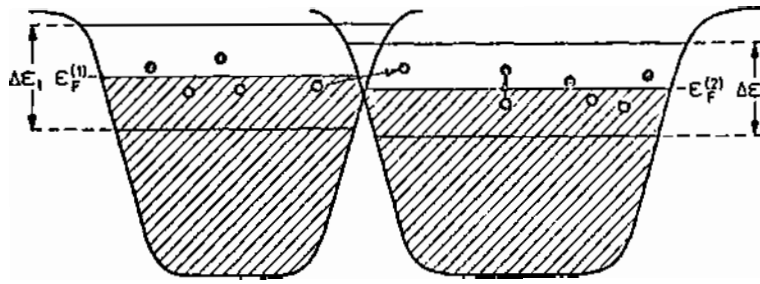

Fig. 5 Schematic illustration of the single-particle model used to evaluate the transport coefficients. The quantities $\Delta\varepsilon$ represent the ranges of single-particle states around the Fermi surface ε_F which are taken into account (From [14]).

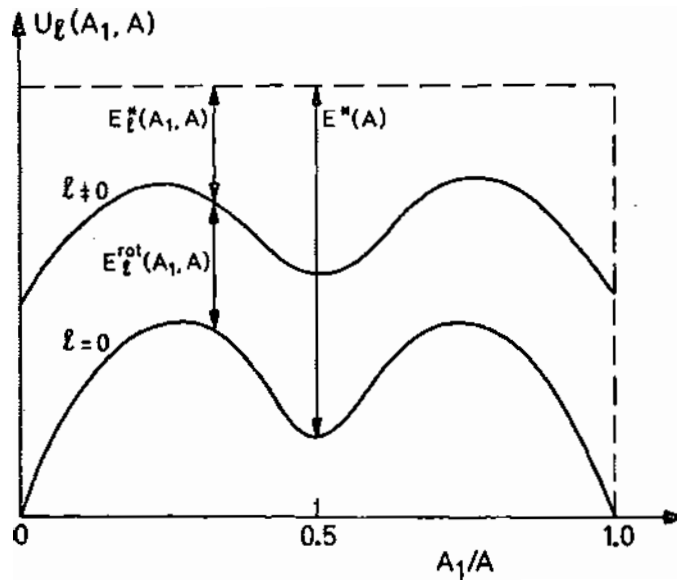

Fig. 6 Illustration of the driving potential $U_{\ell H}(A_1)$, the local excitation energy $E^*_{\ell H}(A_1)$ and the independent variable E^* for fixed total mass A of the system. (From [14]).

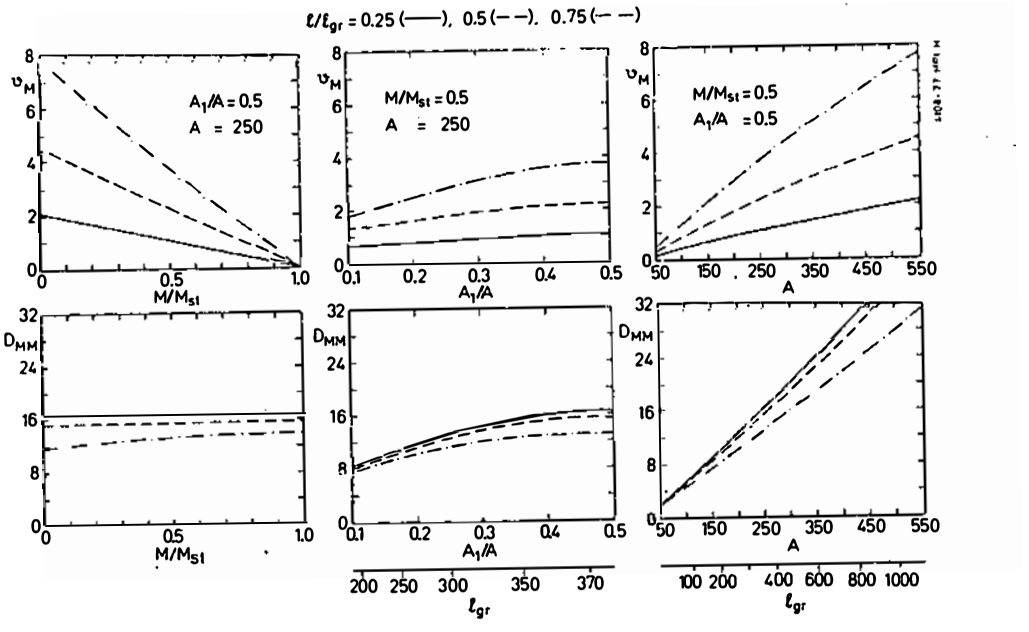

Fig. 7 Drift coefficients υ_M and diffusion coefficients D_{MM} for angular momentum dissipation in units of $10^{22} s^{-1}$. The dependence on internal angular momentum M/M_{st}, mass asymmetry A_1/A and total mass A is shown for different values of the initial relative angular momentum ℓ/ℓ_{gr}. The excitation energy is E^*/A = 1 MeV. (From [15]).

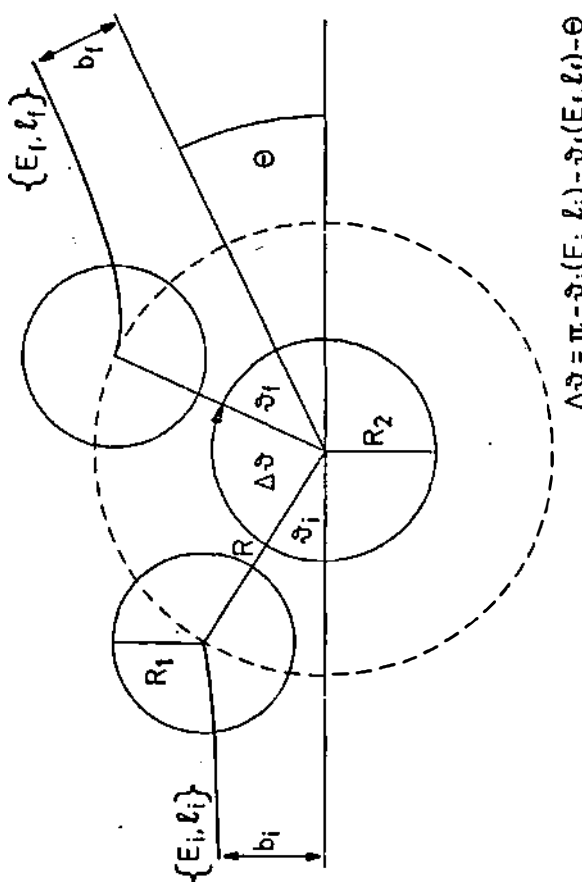

Fig. 8 Illustration of the classical model for the calculation of the mean interaction time in deeply inelastic heavy ion collisions. The Coulomb trajectories shown are for the Kr + Ho reaction described in the text (b_i = 6 fm, b_f = 5.1 fm). (From [12]).

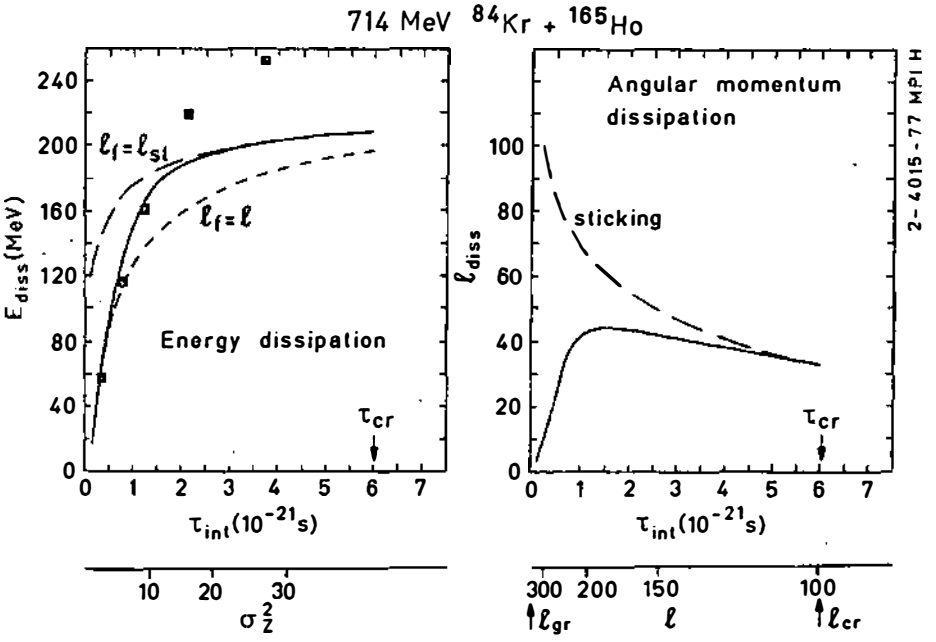

Fig. 9 Energy and angular momentum dissipation as functions of mean interaction time τ_{int}, or initial relative angular momentum ℓ in the Kr + Ho reaction. The experimental points are obtained from the measured energy loss as function of the variance σ_z^2 of the element distribution. The solid curve has been fitted to reproduce the measured energy loss (From [12]).

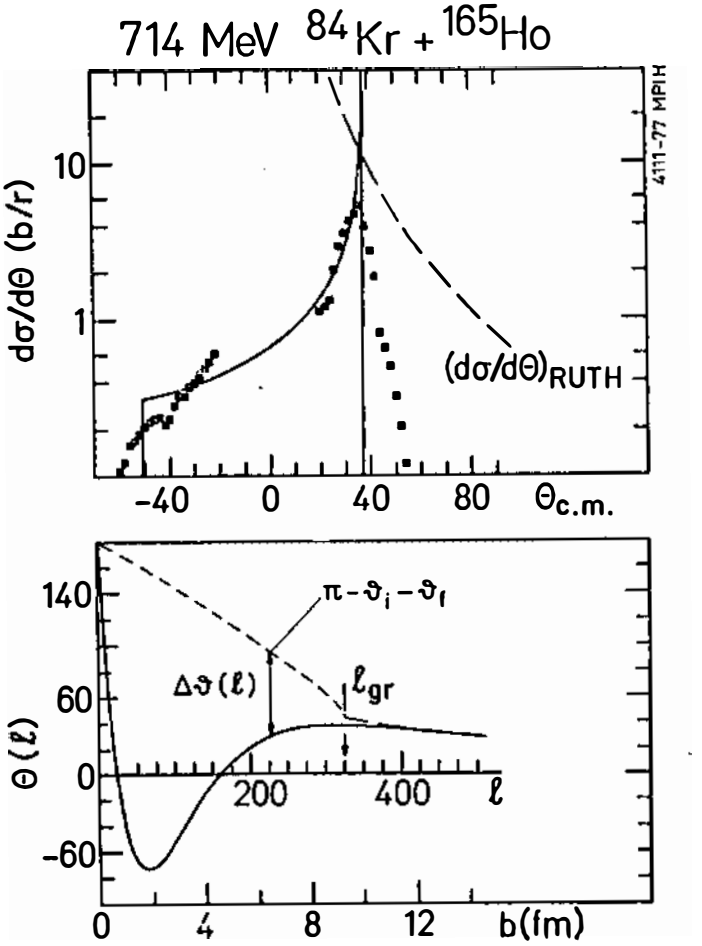

Fig. 10 Determination of the mean deflection function $\Theta(\ell)$ from the experimental angular distribution [21] in the Kr + Ho reaction. For the low ℓ-values $\ell \leq 100$ complete fusion occurs (From [12]).

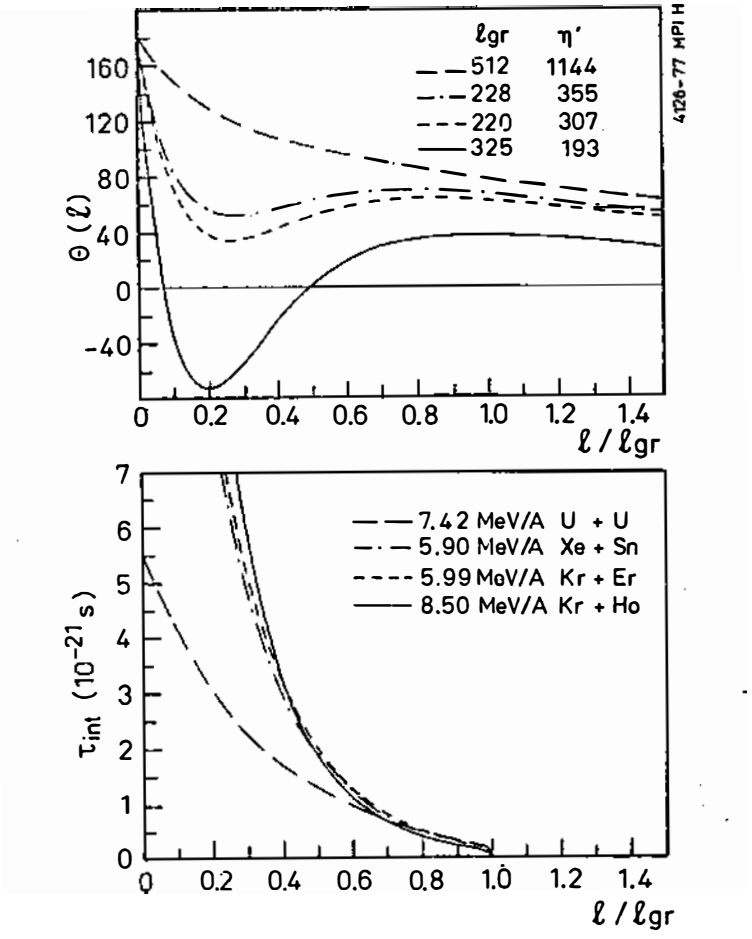

Fig. 11 Mean deflection functions as deduced from the experimental angular distributions for the reactions U + U, Xe + Sn, Kr + Er and Kr + Ho and calculated interaction times as functions of ℓ/ℓ_{gr}. The grazing angular momenta ℓ_{gr} as obtained from quarter-point analyses of elastic scattering data [3,25] and the modified Sommerfeld parameter η' are indicated. The corresponding parameters of the deflection functions are δ = 3, 17.5, 22, 80 and α = 0.10, 0.11, 0.12, 0.18 (From [23]).

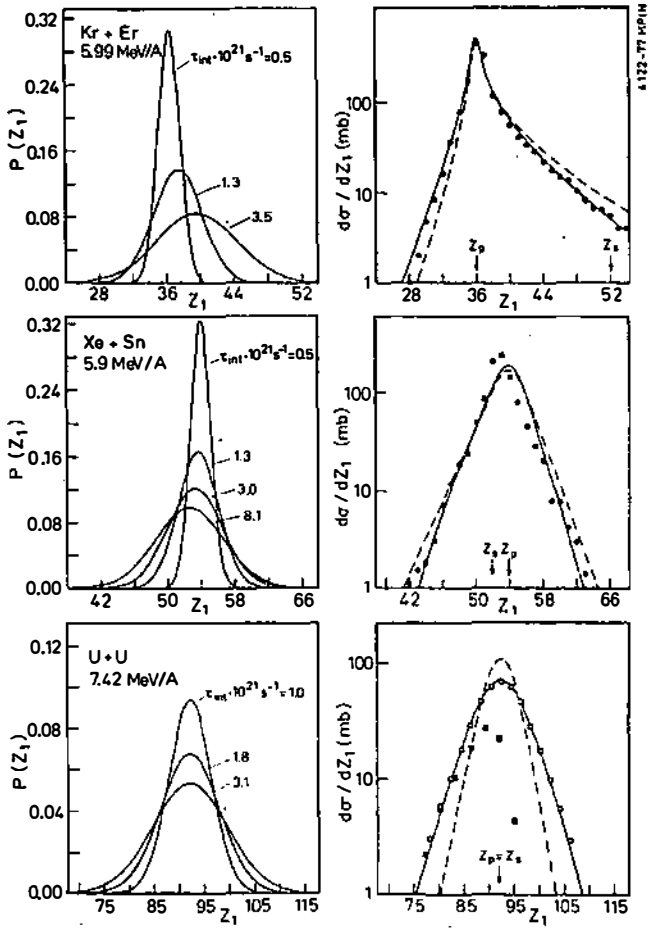

Fig. 12 Element distributions for deeply inelastic collisions. Several solutions $P(Z_1, t)$ of the Fokker-Planck equation are shown. The dashed curves are calculated using the theoretical values for drift and diffusion coefficients, whereas the experimental values of the transport coefficients are deduced from the solid curves. Experimental data are from Gobbi et al. [3] for Kr + Er, Xe + Sn and from Hildenbrand et al. [25] for U + U.

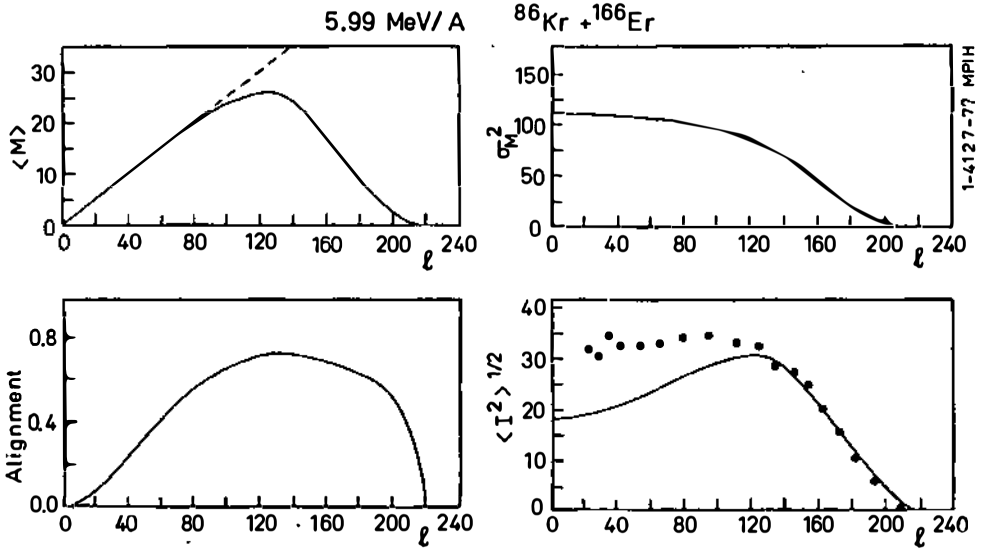

Fig. 13 Upper half: Mean value and variance of the internal angular momentum component M as functions of the initial relative angular momentum ℓ calculated for the Kr + Er reaction. The dashed curve indicates the sticking limit.
Lower half: Alignment and mean absolute value of the total internal angular momentum of the composite system. See text for the comparision with the data points of Gobbi et al. [27].

DISCUSSION

K. Dietrich: There are experimental indications (experiments on circular polarization of the emitted γ-rays and on the angular distribution of the fragments from sequential fission of quasi-uranium) that the alignment of the intrinsic spins of the reaction products in the direction perpendicular to the reaction plane fades away as the energy loss incieases. Does your theory predict this effect?

G. Wolschin: Yes. According to our calculation, the alignment of the internal angular momentum of the composite system along the direction perpendicular to the reaction plane is rather large for most of the partial waves, but decreases towards zero as the initial relative angular momentum approaches zero (i.e., as the energy loss increases). This can be seen in the last figure of my talk.

H. Hofmann: 1) In computing the reaction time you assume the system to rotate at $r = R_o$ which is smaller than R for the interaction barrier (scisson configuration) by about 2 fm. So you neglect the time the system needs to move from R_o to R in the outgoing channel. But in this stage a considerable mass exchange might still take place.

2) To my feeling a realistic description of the excitation of intrinsic angular momentum M is possible only by describing consistently the loss of relative angular momentum l. The parametrization of the deflection function you are using corresponds to a tangential friction force given by a sum of l^2 and l-terms (this is easily derived from the relations of $\Delta\vartheta$ and l_f as well as τ_{int}). The differential equation for the mean value $\langle M \rangle_t$, on the other hand, is at most linear in $\langle M \rangle_t$, as you have shown.